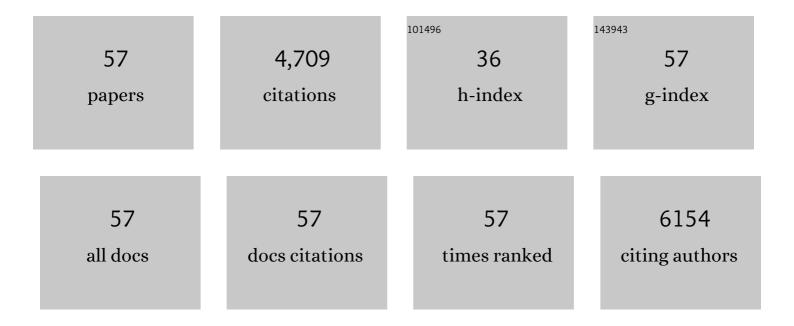
Guangle Niu

List of Publications by Year in descending order

Source: https://exaly.com/author-pdf/4982849/publications.pdf Version: 2024-02-01



CHANCLE NUL

#	Article	IF	CITATIONS
1	A graphene quantum dot photodynamic therapy agent with high singlet oxygen generation. Nature Communications, 2014, 5, 4596.	5.8	1,141
2	Two-photon-excited near-infrared emissive carbon dots as multifunctional agents for fluorescence imaging and photothermal therapy. Nano Research, 2017, 10, 3113-3123.	5.8	246
3	Tunable multicolor carbon dots prepared from well-defined polythiophene derivatives and their emission mechanism. Nanoscale, 2016, 8, 729-734.	2.8	176
4	Exploration of biocompatible AlEgens from natural resources. Chemical Science, 2018, 9, 6497-6502.	3.7	167
5	Functionalized Acrylonitriles with Aggregation-Induced Emission: Structure Tuning by Simple Reaction-Condition Variation, Efficient Red Emission, and Two-Photon Bioimaging. Journal of the American Chemical Society, 2019, 141, 15111-15120.	6.6	155
6	Specific Two-Photon Imaging of Live Cellular and Deep-Tissue Lipid Droplets by Lipophilic AIEgens at Ultralow Concentration. Chemistry of Materials, 2018, 30, 4778-4787.	3.2	154
7	Simultaneous Two-Color Visualization of Lipid Droplets and Endoplasmic Reticulum and Their Interplay by Single Fluorescent Probes in Lambda Mode. Journal of the American Chemical Society, 2021, 143, 3169-3179.	6.6	154
8	Phage-Guided Targeting, Discriminative Imaging, and Synergistic Killing of Bacteria by AIE Bioconjugates. Journal of the American Chemical Society, 2020, 142, 3959-3969.	6.6	143
9	Benzothiazole-Based AlEgen with Tunable Excited-State Intramolecular Proton Transfer and Restricted Intramolecular Rotation Processes for Highly Sensitive Physiological pH Sensing. ACS Sensors, 2018, 3, 920-928.	4.0	136
10	Near-Infrared Probe Based on Rhodamine Derivative for Highly Sensitive and Selective Lysosomal pH Tracking. Analytical Chemistry, 2017, 89, 1922-1929.	3.2	134
11	AIE luminogens as fluorescent bioprobes. TrAC - Trends in Analytical Chemistry, 2020, 123, 115769.	5.8	133
12	Gold nanorod@silica-carbon dots as multifunctional phototheranostics for fluorescence and photoacoustic imaging-guided synergistic photodynamic/photothermal therapy. Nanoscale, 2016, 8, 13067-13077.	2.8	126
13	Coumarin- and Rhodamine-Fused Deep Red Fluorescent Dyes: Synthesis, Photophysical Properties, and Bioimaging in Vitro. Journal of Organic Chemistry, 2013, 78, 6121-6130.	1.7	120
14	Near-Infrared Organic Dye-Based Nanoagent for the Photothermal Therapy of Cancer. ACS Applied Materials & Interfaces, 2016, 8, 29899-29905.	4.0	111
15	Reaction-free and MMP-independent fluorescent probes for long-term mitochondria visualization and tracking. Chemical Science, 2019, 10, 1994-2000.	3.7	83
16	Highly photostable two-photon NIR AIEgens with tunable organelle specificity and deep tissue penetration. Biomaterials, 2019, 208, 72-82.	5.7	82
17	Bright solid-state red-emissive BODIPYs: facile synthesis and their high-contrast mechanochromic properties. Journal of Materials Chemistry C, 2019, 7, 3471-3478.	2.7	81
18	Bright Aggregation-Induced Emission Nanoparticles for Two-Photon Imaging and Localized Compound Therapy of Cancers. ACS Nano, 2020, 14, 16840-16853.	7.3	72

GUANGLE NIU

#	Article	IF	CITATIONS
19	Highly Efficient Aggregation-Induced Red-Emissive Organic Thermally Activated Delayed Fluorescence Materials with Prolonged Fluorescence Lifetime for Time-Resolved Luminescence Bioimaging. ACS Applied Materials & Interfaces, 2020, 12, 51293-51301.	4.0	63
20	Coumarin-Based Boron Complexes with Aggregation-Induced Emission. Journal of Organic Chemistry, 2017, 82, 3456-3462.	1.7	58
21	Near-Infrared Light-Triggered Lysosome-Targetable Carbon Dots for Photothermal Therapy of Cancer. ACS Applied Materials & Interfaces, 2021, 13, 53610-53617.	4.0	54
22	Single Nearâ€Infrared Emissive Polymer Nanoparticles as Versatile Phototheranostics. Advanced Science, 2017, 4, 1700085.	5.6	53
23	<i>In vivo</i> monitoring of tissue regeneration using a ratiometric lysosomal AIE probe. Chemical Science, 2020, 11, 3152-3163.	3.7	52
24	Water-Soluble Polythiophene for Two-Photon Excitation Fluorescence Imaging and Photodynamic Therapy of Cancer. ACS Applied Materials & Interfaces, 2017, 9, 14590-14595.	4.0	49
25	A colorimetric and fluorescent lighting-up sensor based on ICT coupled with PET for rapid, specific and sensitive detection of nitrite in food. Chemical Communications, 2019, 55, 9947-9950.	2.2	48
26	Exploiting the Twisted Intramolecular Charge Transfer Effect to Construct a Wash-Free Solvatochromic Fluorescent Lipid Droplet Probe for Fatty Liver Disease Diagnosis. Analytical Chemistry, 2022, 94, 3881-3887.	3.2	48
27	Single AlEgen for multiple tasks: Imaging of dual organelles and evaluation of cell viability. Biomaterials, 2020, 242, 119924.	5.7	46
28	A Single Fluorescent pH Probe for Simultaneous Two-Color Visualization of Nuclei and Mitochondria and Monitoring Cell Apoptosis. ACS Sensors, 2021, 6, 1552-1559.	4.0	46
29	A pH-Sensitive Spirocyclization Strategy for Constructing a Single Fluorescent Probe Simultaneous Two-Color Visualizing of Lipid Droplets and Lysosomes and Monitoring of Lipophagy. Analytical Chemistry, 2021, 93, 11729-11735.	3.2	46
30	Cancer cell discrimination and dynamic viability monitoring through wash-free bioimaging using AlEgens. Chemical Science, 2020, 11, 7676-7684.	3.7	45
31	Deep-Red Emissive Crescent-Shaped Fluorescent Dyes: Substituent Effect on Live Cell Imaging. ACS Applied Materials & Interfaces, 2015, 7, 7421-7427.	4.0	44
32	Graphene quantum dots as efficient, metal-free, visible -light-active photocatalysts. Science China Materials, 2016, 59, 12-19.	3.5	44
33	Deep-Red and Near-Infrared Xanthene Dyes for Rapid Live Cell Imaging. Journal of Organic Chemistry, 2016, 81, 7393-7399.	1.7	43
34	Simultaneous visualization of lipid droplets and lysosomes using a single fluorescent probe. Sensors and Actuators B: Chemical, 2021, 329, 129148.	4.0	41
35	Aminobenzofuran-Fused Rhodamine Dyes with Deep-Red to Near-Infrared Emission for Biological Applications. Journal of Organic Chemistry, 2015, 80, 3170-3175.	1.7	40
36	Polymer nanoparticles with high photothermal conversion efficiency as robust photoacoustic and thermal theranostics. Journal of Materials Chemistry B, 2017, 5, 2832-2839.	2.9	37

GUANGLE NIU

#	Article	IF	CITATIONS
37	Lysosome-targetable polythiophene nanoparticles for two-photon excitation photodynamic therapy and deep tissue imaging. Journal of Materials Chemistry B, 2017, 5, 3651-3657.	2.9	36
38	Versatile Polymer Nanoparticles as Twoâ€Photonâ€Triggered Photosensitizers for Simultaneous Cellular, Deepâ€Tissue Imaging, and Photodynamic Therapy. Advanced Healthcare Materials, 2017, 6, 1601431.	3.9	35
39	Ketoâ€benzo[<i>h</i>]â€Coumarinâ€Based Nearâ€Infrared Dyes with Large Stokes Shifts for Bioimaging Applications. Chemistry - an Asian Journal, 2016, 11, 498-504.	1.7	34
40	In Vitro Lightâ€Up Visualization of a Subunitâ€Specific Enzyme by an AIE Probe via Restriction of Single Molecular Motion. Angewandte Chemie - International Edition, 2020, 59, 10003-10007.	7.2	34
41	A family of multi-color anthracene carboxyimides: Synthesis, spectroscopic properties, solvatochromic fluorescence and bio-imaging application. Dyes and Pigments, 2017, 139, 166-173.	2.0	32
42	Acceptor-donor-acceptor structured deep-red AIE photosensitizer: Lysosome-specific targeting, in vivo long-term imaging, and effective photodynamic therapy. Chemical Engineering Journal, 2022, 430, 132638.	6.6	28
43	Fluorescent AIE-Active Materials for Two-Photon Bioimaging Applications. Frontiers in Chemistry, 2020, 8, 617463.	1.8	27
44	Ratiometric Detection of Mitochondrial Thiol with a Two-Photon Active AlEgen. ACS Applied Bio Materials, 2019, 2, 3120-3127.	2.3	26
45	Visualizing semipermeability of the cell membrane using a pH-responsive ratiometric AIEgen. Chemical Science, 2020, 11, 5753-5758.	3.7	26
46	Diagnosis of fatty liver disease by a multiphoton-active and lipid-droplet-specific AlEgen with nonaromatic rotors. Materials Chemistry Frontiers, 2021, 5, 1853-1862.	3.2	22
47	Specific photoacoustic cavitation through nucleus targeted nanoparticles for high-efficiency tumor therapy. Nano Research, 2020, 13, 719-728.	5.8	21
48	Selectively light-up hydrogen peroxide in hypoxic cancer cells with a novel fluorescent probe. Chemical Communications, 2018, 54, 13957-13960.	2.2	18
49	Precise and long-term tracking of mitochondria in neurons using a bioconjugatable and photostable AlE luminogen. Chemical Science, 2022, 13, 2965-2970.	3.7	18
50	Mitochondria-targeting NIR fluorescent probe for rapid, highly sensitive and selective visualization of nitroxyl in live cells, tissues and mice. Science China Chemistry, 2020, 63, 282-289.	4.2	16
51	Deep-red to near-infrared fluorescent dyes: Synthesis, photophysical properties, and application in cell imaging. Spectrochimica Acta - Part A: Molecular and Biomolecular Spectroscopy, 2016, 164, 8-14.	2.0	15
52	Red emissive fluorescent probe for the rapid detection of selenocysteine. Sensors and Actuators B: Chemical, 2018, 264, 234-239.	4.0	15
53	Polarized resonance synchronous spectroscopy as a powerful tool for studying the kinetics and optical properties of aggregation-induced emission. Journal of Materials Chemistry C, 2019, 7, 12086-12094.	2.7	11
54	Two-Color Visualization of Cholesterol Fluctuation in Plasma Membranes by Spatial Distribution-Controllable Single Fluorescent Probes. Analytical Chemistry, 2021, 93, 9074-9082.	3.2	10

#	Article	IF	CITATIONS
55	In Vitro Lightâ€Up Visualization of a Subunitâ€Specific Enzyme by an AIE Probe via Restriction of Single Molecular Motion. Angewandte Chemie, 2020, 132, 10089-10093.	1.6	6
56	A water-soluble and photostable aggregation-induced emission lumogen for imaging Gram-negative bacteria by supramolecular assembly. Dyes and Pigments, 2021, 194, 109653.	2.0	6
57	Fabrication of small-structure red-emissive fluorescent probes for plasma membrane enables quantification of nuclear to cytoplasmic ratio in live cells and tissues. Spectrochimica Acta - Part A: Molecular and Biomolecular Spectroscopy, 2021, 249, 119338.	2.0	2